

Optical characterization of electronic transitions arising from the Au/S interface of self-assembled *n*-alkanethiolate monolayers

J. Shi ^{a,1}, B. Hong ^b, A.N. Parikh ^a, R.W. Collins ^c, D.L. Allara ^d

^a Department of Materials Science and Engineering, Pennsylvania State University, University Park, PA 16802, USA

^b Department of Electrical Engineering, Pennsylvania State University, University Park, PA 16802, USA

^c Department of Physics, Pennsylvania State University, University Park, PA 16802, USA

^d Department of Chemistry, Pennsylvania State University, University Park, PA 16802, USA

Received 2 August 1995

Abstract

Analyses of optical frequency ellipsometric spectra obtained in situ upon completion of the self-assembly of *n*-alkanethiolate monolayers on gold substrates immersed in methanol reveal the presence of a 1.2 ± 0.4 Å thick S/Au interface layer. This layer exhibits unique optical transitions, modeled as two Lorentzian oscillators with imaginary parts peaked at ≈ 570 nm (≈ 2.2 eV) and ≈ 290 nm (≈ 4.3 eV), indicating a perturbation of the near-surface gold electronic structure upon thiol chemisorption. A further, more rigorous, spectral analysis involving an anisotropic, uniaxially oriented chain assembly reveals the presence of significant microscopic void defects in the otherwise densely packed monolayers.

Self-assembled monolayers (SAMs) of alkanethiolates on gold [1] have generated increasing interest over the past several years and extensive efforts have been made to characterize these films [2]. While considerable effort has been directed towards determining the molecular structure and the chain organization [2], little is known about the S/Au interface. Electronic structure calculations [3] based on 16 Au-atom clusters show that the chemisorption of a CH₃S species at a (111) hollow site involves the formation of an ≈ 1.9 Å surface dipole layer via transfer of ≈ 0.4 of an electron to the S with the

positive residual charge delocalized among several Au atoms. Direct experimental characterization of this layer is vital for establishing a firm understanding of the nature of the S–Au chemisorptive interaction [2–4] and for providing a more complete physical description of these SAMs. In this Letter we apply ellipsometric spectroscopy measurements, coupled with quantitative analyses involving electromagnetic theory, to provide the first accurate experimental characterization of the S/Au interface layer in well-formed monolayers for the particular case of *n*-alkanethiolates, C_{*n*}H_{2*n*+1}S– with *n* between 10 and 22. These data show the existence of unique optical transitions localized in an ≈ 1.2 Å interface layer, independent of the alkanethiolate chain length. In addition, a preliminary analysis of the spectra for

¹ Present address: Fusion Systems Corporation, 7600 Standish Place, Rockville, MD 20855, USA.

the C_{18} SAM, in terms of domains of densely packed, oriented, optically anisotropic chains, further shows that void defects are intrinsic to well-formed SAMs.

Freshly deposited Au (≈ 200 nm; 99.999%)/Cr (≈ 9 nm)/Si(native oxide) samples were immersed immediately in high purity methanol and stored until use. Surface contamination was minimized by conducting the experiments in situ, i.e. directly in the presence of solvent. The samples were mounted in the optical cell with continual solvent washing until the cell was filled. The cell was fabricated from a solid cylinder of strain-free, vitreous silica and corrective cylindrical lenses were mounted externally in order to maintain beam collimation throughout the optical path. After optical alignment, bare Au film measurements were made, a measured aliquot of a concentrated methanolic alkanethiol solution was added and, finally, spectra were taken over 18–24 h immersion. Complete spectral sets were obtained for the thiols with even C numbers 10–22. The instrument was an in-house modified, commercial (SOPRA, Bois-Colombes, France) rotating-polarizer instrument (56 Hz) set at a 70° incidence angle and calibrated using established procedures [5,6]. The modulated signal intensities were characterized by a Hadamard-type analysis [7] to generate the conventional ellipsometry parameters Ψ and Δ [8].

Representative Ψ and Δ difference spectra for the C_{10} , C_{16} and C_{22} SAMs, calculated as difference between the $\text{CH}_3\text{OH}/\text{SAM}/\text{Au}$ and the $\text{CH}_3\text{OH}/\text{Au}$ spectra, are given in Fig. 1. The bare Au spectra reproduce ones previously reported [9] and are not shown. The entire set of spectra were analyzed by performing numerical simulations, based on standard laminar model structures with mathematically sharp interfaces. Systematic changes in sample parameters were varied until satisfactory agreement between experiment and simulation was reached using a previously reported error criterion [9].

In the models, the j th layer of the laminar structure consists of a uniform material of thickness d_j and frequency-dependent complex dielectric function $\hat{\epsilon}^j(\nu) = \epsilon^j(\nu) + i\epsilon_2^j(\nu)$ or, alternatively, complex optical function $\hat{n}^j(\nu) = n^j(\nu) + ik^j(\nu)$, where $\hat{\epsilon}^j = (\hat{n}^j)^2$. For isotropic and anisotropic optical responses, $\hat{\epsilon}^j$ and \hat{n}^j are represented by scalars and second rank tensors (designated $\tilde{\epsilon}^j$ and \tilde{n}^j), respec-

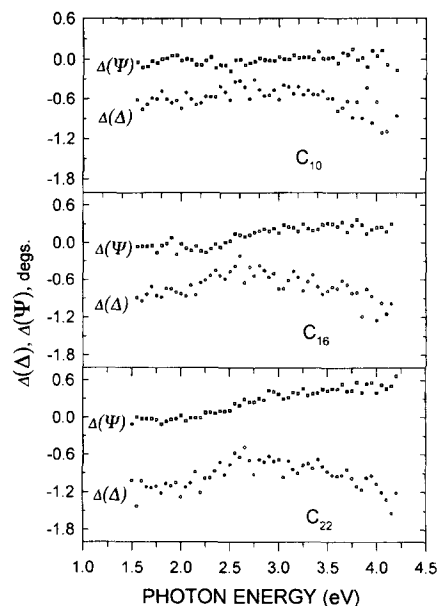


Fig. 1. Representative Ψ , Δ difference spectra (SAM – bare Au) versus photon energy for $C_n\text{H}_{2n+1}\text{SH}$ SAM films with $n = 10, 16$ and 22 .

tively. Our major analysis concentrates on an isotropic SAM model; later in the report we present a preliminary treatment of anisotropic structures. The associated relationships used to calculate Ψ and Δ spectra are described in detail elsewhere for the cases of both isotropic [8,9], and anisotropic [10,11] models.

Simulations were carried out using a 4-medium model, $\text{CH}_3\text{OH}(\epsilon^0)/\text{SAM}(\hat{\epsilon}^f, d_i^{(n)})/\text{interface}(\hat{\epsilon}^{(n)\text{int}}(\nu), d_{\text{int}}^{(n)})/\text{Au}(\hat{\epsilon}^{\text{Au}}(\nu))$, where the ϵ and d values are the layer dielectric functions and thicknesses, respectively, and the superscript n designates a dependence on the total carbon number of the alkanethiol. The input values of ϵ^0 and $\hat{\epsilon}^{\text{Au}}(\nu)$ were determined independently. The other parameters were determined by iterative fitting procedures with the realistic physical constraint imposed that $\hat{\epsilon}^f(\nu)$, or equivalently, $\hat{n}^f(\nu)$, possesses only a single, chain length independent, real value. The latter constraint is based on the fact that the alkanethiols used are non-absorbing in the 350–850 nm range with negligible frequency dispersion in $\text{Re}(\hat{n})$ and that the crystalline forms have nearly identical refractive indices.

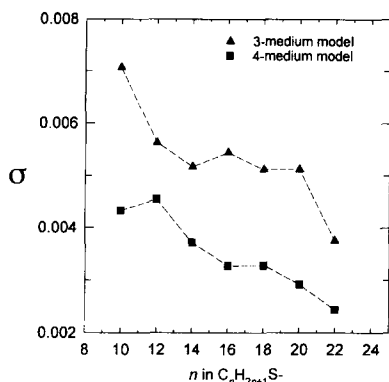


Fig. 2. Unbiased, mean square deviation errors between experiment and simulation obtained for analyses without (\blacktriangle) and with (\blacksquare) a S/Au interface layer.

Regression analysis of the SAM spectral set (C_{10} – C_{22}) without the interface layer gave a slight minimum in the global fitting error [9] for $n^f = 1.50(\pm 0.01; 95\% \text{ confidence limits})$ and also gave the SAM thickness–C number dependence: $d_{\text{int}}^{(n)} = sn + d_0$ with $s = 1.21 \text{ \AA}/C$ and $d_0 = 0.6 \text{ \AA}$. The minimum fitting error is shown in Fig. 2 where it can be seen that addition of a S/Au interface layer improves fits for all chain lengths. Further, as discussed below, the above value of d_0 is physically unrealistic compared to that derived from a model which includes an interface layer.

The most general analysis with the interface layer includes both chemisorption-induced interface roughness and electronic perturbations. Trial runs with different roughness models showed negligible improvement of fits. The electronic perturbations were modeled by starting from the 3-medium analysis values of $d_{\text{int}}^{(n)}$ and n^f , and sets of $\hat{\epsilon}^{(n)\text{int}}(\nu)$ spectra were generated for trial $d_{\text{int}}^{(n)}$ values by exact mathematical inversion [12]. The validity of the $\hat{\epsilon}^{(n)\text{int}}(\nu)$ spectra were judged by the physically realistic criteria² that they show no artifacts from the Au dielectric functions, obey the Kramers–Kronig (KK) relations and exhibit a gradual drop of the real part to zero at the lowest photon energies, a behavior generally expected for electromagnetic wave interactions with electrons in localized states at the interface. Adherence to all the above criteria were met only for

$d_{\text{int}}^{(n)}$ values of $\approx 1 \text{ \AA}$. The final sets of interface layer dielectric function spectra $\{\hat{\epsilon}^{(n)\text{int}}(\nu)\}$ were obtained via a combination of regression and exact inversion procedures on the complete $\{\Psi^{(n)}(\nu), \Delta^{(n)}(\nu)\}$ experimental spectral set.

A representative $\hat{\epsilon}^{(n)\text{int}}(\nu)$ spectrum, for $n = 10$ with an associated layer thickness of 1.4 \AA , is shown in Fig. 3. The features in the spectra are physically realistic since they appear in both the dispersive part (as a step) and the absorptive part (as a peak). More quantitatively, these features are consistent with the required causal KK behavior as shown by the ability to fit the data to the damped harmonic oscillator expression [14]

$$\hat{\epsilon}(E) = n_0^2 + \sum_{j=1}^{N_0} \frac{F_j^2}{(E_j^2 - E^2) - iE\Gamma_j}, \quad (1)$$

which strictly obeys the KK relations. In Eq. (1), $\hat{\epsilon}(E)$ is the dielectric function at energy $E = h\nu$; E_j , F_j and Γ_j represent the resonance energies, oscillator strengths, and linewidth parameters, respectively, for the j th oscillator of the set of N_0 oscillators; and n_0 represents the high-frequency index of refraction which may be larger than unity due to non-resonant contributions and to undetected resonances at high energies. The solid lines in Fig. 3 show the best fit to Eq. (1) using $E_1 = 2.30$ and $E_2 = 4.05 \text{ eV}$. The average (E , Γ , F) values for the two transitions, in units of eV, obtained from the complete SAM set are 2.2, 0.62, 1.0 and 4.3, 2.0, 1.2. These values lead to

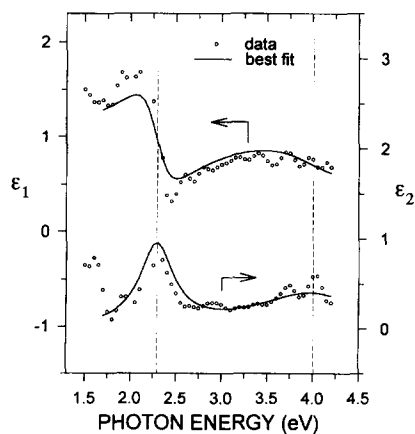


Fig. 3. Interface dielectric function spectra of $C_nH_{2n+1}S-/Au$ SAMs, for $n = 10$, obtained from the Ψ , Δ spectra. The solid lines represent a Lorentzian oscillator fit as described in the text.

² For an overview of some of these methods, see Ref. [13].

the average, chain length-independent values of $1.48 < n^f < 1.52$, with a slight minimum around 1.50, and $1.0 \leq d_{\text{int}} \leq 1.4 \text{ \AA}$. The corresponding improvements in the experimental fits, as shown in Fig. 2, by using this average interface dielectric function, shows the existence of a unique, electronically perturbed interface layer.

The SAM thicknesses which result from the inclusion of the average interface characteristics in the data analyses follow the linear correlation $d_{\text{f}}^{(n)} = sn + d_0$ with $d_0 = 1.94 \text{ \AA}$ and $s \approx 1.19 \text{ \AA/C}$. The value of d_0 corresponds quite closely to the expected size of the residual S atom on a zero carbon chain, as opposed to $d_0 = 0.6 \text{ \AA}$ obtained from the analysis without the interface layer (see above) while $s \approx 1.19 \text{ \AA/C}$ corresponds roughly to the expected slope of 1.10 required for $\approx 28^\circ$ tilted chains [2,15]. This analysis indicates that the S/Au interface is localized in a region between the tops of the Au surface atoms and the bottom of the sulfur, a location consistent with the perturbed electron density of states which should arise at the gold surface upon dissociative chemisorption of the thiol. The general correspondence between the theoretical thickness of $\approx 1.9 \text{ \AA}$ for this dipole layer [3], and our average value of $d_{\text{int}} \approx 1.2 \text{ \AA}$ further supports this structure. While our data show that discrete optical transitions are associated with the S/Au interfacial layer, it is not clear presently whether these transitions arise from a localized or delocalized electronic configuration, and it would appear that further work is needed to identify the detailed excitation mechanism(s), e.g. discrete electronic transitions or dipolar plasmon resonances.

We find that with the nature of the interface layer defined, it is possible to isolate other aspects of the film structures, and here we briefly address the important issue of density. Since the above average best-fit value of $n^f \approx 1.50$ is lower than the highest value of 1.53 reported for the densest alkyl phases of crystalline polyethylene [16], it appears that the SAM matrices, even in our highly organized films, contain microscopic voids. As a preliminary step, we have modeled the C_{18} SAM in terms of a more realistic structure with $\approx 5\text{--}15 \text{ nm}$ [17,18] domains of oriented chains of tilt angle φ (defined relative to the surface normal) [2,15], rather than a uniform isotropic medium with no directional characteristics, as used above. The directionality and density discrepancy

were incorporated, respectively, by treating the refractive index as a tensor, $\vec{n}^f(\varphi, \nu)$ with uniaxial symmetry and by applying the Maxwell–Garnett approximation [19] to calculate the effective dielectric function for variable void contents in which the voids were filled with either methanol solvent or disordered, liquid-like chains with an isotropic refractive index of ≈ 1.44 . The matrix elements, $n_{ij}^f(\varphi)$, were calculated independently using den Engelson's Lorentz cavity method [20] and adjusted to $\varphi = 28^\circ$ using a rotation operator.

Using a previously reported algorithm [11], simulations were carried out for the C_{18} SAM at four widely spaced wavelength points, and the best-fit values of the SAM void fractions, f_v , were deduced. The results show that any attempt to match the experimental data without void content in the SAM layer leads to physically unreasonable film thicknesses and that the best global fit over the four wavelength points is obtained with $f_v \approx 4\text{--}10\%$ or $8\text{--}20\%$ for incorporation of either methanol or disordered alkyl chains into the voids, respectively. These values of defect populations are quite realistic in view of the mixed morphologies present in vapor-deposited Au films and also are consistent with the intrinsic void content observed as surface depressions in recently reported scanning tip microscopy images of alkanethiolate/Au SAMs [21–23]. Further work is now underway in our laboratories to obtain more accurate characterizations of the film matrix and the S/Au interface, including their time evolution during assembly, by the use of higher signal/noise measurements, single crystal substrates, and variation of the assembling solvent.

Acknowledgements

Financial support was provided by the National Science Foundation under Grant Nos. DMR 9001270 (DLA and ANP), DMR-8957159 (BH and RWC) and DMR-9217169 (RWC). Discussions with M.J. Natan are gratefully acknowledged.

References

- [1] A. Ulman, An introduction to ultrathin organic films, from Langmuir–Blodgett to self-assembly (Academic, New York, 1991).

- [2] L.H. Dubois and R.G. Nuzzo, *Ann. Rev. Phys. Chem.* 43 (1992) 437.
- [3] H. Sellers, A. Ulman, Y. Shnidman and J. Eilers, *J. Am. Chem. Soc.* 115 (1993) 9389.
- [4] P. Fenter, A. Ederhardt and P. Eisenberger, *Science* 266 (1994) 1216.
- [5] R.W. Collins, *Proc. SPIE* 617 (1986) 62.
- [6] D.E. Aspnes, *J. Opt. Soc. Am.* 64 (1974) 812.
- [7] G. Laurence, F. Hottier and J. Hallais, *Rev. Phys. Appl. (Paris)* 16 (1981) 579.
- [8] R.M.A. Azzam and N.M. Bashara, *Ellipsometry and polarized light* (North-Holland, Amsterdam, 1977).
- [9] Y.T. Kim, R.W. Collins, K. Vedam and D.L. Allara, *J. Electrochem. Soc.* 138 (1991) 3266.
- [10] D.L. Allara and A.N. Parikh, *J. Chem. Phys.* 96 (1992) 927.
- [11] A.N. Parikh and D.L. Allara, *Optical studies on real surfaces and films*, in: *Physics of thin films series*, Vol. 19, eds. M. Francombe and J.L. Vossen (Academic, New York, 1994).
- [12] W.G. Oldham, *Surface Sci.* 16 (1969) 97.
- [13] D.E. Aspnes, *Proc. SPIE* 946 (1988) 84.
- [14] R.W. Collins and K. Vedam, in: *Encyclopedia of Applied Physics*, Vol. 12, ed. G. Trigg (VCH, Weinheim, 1995) p. 298.
- [15] P.E. Laibinis, G.M. Whitesides, D.L. Allara, Y.-T. Tao, A.N. Parikh and R.G. Nuzzo, *J. Am. Chem. Soc.* 113 (1991) 7152.
- [16] *Polymer handbook*, eds. J. Brandrup and E.H. Immergut, Vol. 13 (Wiley, New York, 1975) p. V-22.
- [17] N. Camillone III, C.E.D. Chidsey, P. Eisenberger, P. Fenter, J. Li, K.S. Liang, G.-Y. Liu and G. Scoles, *J. Chem. Phys.* 99 (1993) 744.
- [18] G.E. Poirier and M.J. Tarlov, *Langmuir* 10 (1994) 2853.
- [19] J.C. Maxwell-Garnett, *Phil. Trans.* 205 (1906) 237.
- [20] D. den Engelsen, *Surface Sci.* 56 (1976) 272.
- [21] Y.-T. Kim and A.J. Bard, *Langmuir* 8 (1992) 1096.
- [22] H.-J. Butt, D. Seifert and E. Bamberg, *J. Phys. Chem.* 97 (1993) 7316.
- [23] K. Edinger, A. Golzhauser, K. Demota, Ch. Wöll and M. Grunze, *Langmuir* 9 (1993) 4.